

On the mobility of all-terrain rovers

Giulio Reina

Department of Engineering for Innovation, University of Salento, Lecce, Italy, and

Mario Foglia

Department of Mechanical and Management Engineering, Politecnico of Bari, Bari, Italy

Abstract

Purpose – The purpose of this paper is to evaluate the locomotion performance of all-terrain rovers employing rocker-type suspension system.

Design/methodology/approach – In this paper, a robot with advanced mobility features is presented and its locomotion performance is evaluated, following an analytical approach via extensive simulations. The vehicle features an independently controlled four-wheel-drive/4-wheel-steer architecture and it also employs a passive rocker-type suspension system that improves the ability to traverse uneven terrain. An overview of modeling techniques for rover-like vehicles is introduced. First, a method for formulating a kinematic model of an articulated vehicle is presented. Next, a method for expressing a quasi-static model of forces acting on the robot is described. A modified rocker-type suspension is also proposed that enables wheel camber change, allowing each wheel to keep an upright posture as the suspension conforms to ground unevenness.

Findings – The proposed models can be used to assess the locomotion performance of a mobile robot on rough-terrain for design, control and path planning purposes. The advantage of the rocker-type suspension over conventional spring-type counterparts is demonstrated. The variable camber suspension is shown to be effective in improving a robot's traction and climbing ability.

Research limitations/implications – The paper can be of great value when studying and optimizing the locomotion performance of mobile robots on rough terrain. These models can be used as a basis for advanced design, control and motion planning.

Originality/value – The paper describes an analytical approach for the study of the mobility characteristics of vehicles endowed with articulated suspension systems. A variable camber mechanism is also presented.

Keywords Robots, Motion, Control systems, Field robotics, Articulated suspension system, Rover modeling, Wheel cambering mechanism

Paper type Research paper

1. Introduction

For mobile robots driving across natural terrain, it is critical to be endowed with an efficient locomotion system. Different solutions have been proposed, including wheel with suspension, leg mechanisms, tracks, and hopping and snake-like systems. All the major types of mobility systems can be broadly classified under the following three categories (Sandin, 2003): wheeled, tracked and legged systems, although numerous hybrid locomotion systems have also been proposed (Rohmer *et al.*, 2010; Quaglia *et al.*, 2011).

Walking robots potentially represent the best locomotion system on rugged terrain, overcoming most of the problems affecting either wheeled or tracked robots. However, legged robots face a number of challenges. Many of these challenges stem from the large number of degrees of freedom that make their cost of building higher relative to those with wheels or tracks; walking mechanisms are also more complex and thus more prone to failure. Furthermore, optimal control of walking

machines is more sophisticated and it is still an active area of research (Remy *et al.*, 2011). Tracked vehicles have demonstrated their better performance over wheeled systems, especially for very soft terrain as deep mud and loose sand (Wong and Huang, 2006). However, they achieve higher mobility at the cost of greater complexity, lower drive efficiency and higher power-to-weight ratio. The steering is obtained by “skid” steering, i.e. by differential driving of the two tracks. Friction within the tracks themselves dissipates energy whenever the vehicle turns because the treads must slip against the ground. Because of the large amount of skidding during a turn, the exact center of rotation of the robot is hard to predict and the exact change in position and orientation is also subject to variations, depending on the ground friction. Therefore, the dead-reckoning ability of tracked vehicles is poor.

The wheel has been by far the most popular locomotion mechanism in mobile robotics for several practical reasons. Wheeled robots are mechanically simple and easy to construct. Both legged and tracked systems generally require more complex and heavier hardware than wheeled systems designed to carry the same payload. The principal disadvantage of wheels is that they may perform poorly on uneven terrain. As a rule of thumb, a wheeled vehicle has trouble if the height of the object it must surmount approaches the radius of the wheels. In order to overcome this issue, an appropriate suspension system may be used. Although the details of automotive suspensions used today are widely varied, they all use some form of spring and

The current issue and full text archive of this journal is available at www.emeraldinsight.com/0143-991X.htm



Industrial Robot: An International Journal
40/2 (2013) 121–131
© Emerald Group Publishing Limited [ISSN 0143-991X]
[DOI 10.1108/014399911311297720]

shock combination to provide good control and a relatively comfortable ride to the driver (Gillespie, 1992). Most suspensions are designed for high-speed control over mostly smooth surfaces, but more importantly, they are designed for human-driven vehicles. Regardless of their popularity and notable performance in race cars and off-road vehicles, there are very few sprung suspension systems adopted in mobile robotics. Springs mainly address drive comfort and control issues in vehicles that travel more than about 8 m/s. Below that speed, they are actually an impediment to mobility since they change the force each wheel exerts on the ground, as obstacles are negotiated. A four-wheeled conventional independent suspension vehicle appears to keep all wheels equally on the ground, but the wheels that are on the bumps, being lifted, are carrying more weight than the other wheels. This reduces the traction of the lightly loaded wheels. A better solution, at low speeds, is to allow some of the wheels to rise, relative to the chassis, over bumps without changing the weight distribution or changing it as little as possible. This objective can be achieved using a passive articulated suspension. A notable example is the so-called rocker-bogie suspension (Bickler, 1998) that has been successfully demonstrated by NASA's rovers Spirit and Opportunity for planetary exploration (Maimone *et al.*, 2004).

According to this solution (Bickler, 1989) and with reference to the robot Dune, shown in Figure 1, that features a four-wheel embodiment of the rocker-bogie suspension, usually simply referred to as rocker suspension, the drive wheels of either side of the vehicle are connected longitudinally by a rigid link, called rocker arm. Each one of the two rockers is pivoted to the main frame of the vehicle through the axis of a differential gearbox, whose input gear is attached to the chassis (Figure 1(b)). This configuration allows the rocker arms to pivot when any wheel tries to go higher or lower than the rest. The passive pivoting action keeps the load on all four wheels almost equal, increasing mobility simply by maintaining driving and braking action on all wheels at all times. Furthermore, the mechanical differential constraints the pitch angle of the chassis to be half of the pitch angle of either rocker. The pitch averaging effectively reduces the pitching motion of the chassis,

maintaining it at a more level pose, as either side of the suspension system travels over obstacles. This is beneficial in vehicles under camera control, and, in general, an autonomous sensor-driven robot can benefit from less rocking motion of the main chassis.

Relatively limited research has been devoted to investigate expressly the locomotion performance of rocker-type rovers (Lindemann and Voorhees, 2005; Thueer *et al.*, 2007; Schäfer *et al.*, 2010). In this paper, the mobility characteristics of Dune are studied following an analytical approach and they are validated via extensive simulations. An overview of modeling techniques for rover-like robots is presented. These models can be used as a basis for advanced design, control and motion planning to improve mobility on uneven terrain. First, a method for formulating a kinematic model of a rover is presented. Then, a method for expressing a quasi-static model of forces acting on the vehicle is described. These models are computationally simple, and, thus, practical for on-board implementation. Based on these models, the motion performance of the rover can be analyzed, demonstrating its advantages over conventional systems.

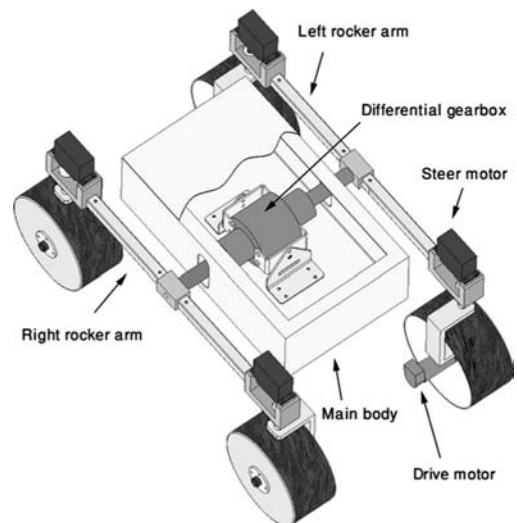
However, one important limitation to the use of rocker-type suspensions is that they do not provide any compensation of wheel inclination angle relative to the ground in the transverse plane, i.e. the camber angle, during suspension travel. This causes the wheels to deviate from their optimal posture, corresponding to a perfectly perpendicular configuration, as the robot adapts to terrain unevenness, thus reducing the traction performance and promoting undesired effects, such as wheel slip and sinkage, which greatly affect mobility (Reina *et al.*, 2006). In addition, vehicle yaw may also be induced producing unpredictable deviations from the intended path. In principle, an upright wheel maximizes its footprint, reducing ground pressure and, therefore, sinkage in soft terrain (Wong, 2001). At the same time, the “grip” of the wheel, i.e. its ability to exchange forces with the ground, increases, thus reducing slippage.

A second main contribution of this work is a variable camber mechanism that can be easily integrated with rocker suspension systems. The idea is to obtain an adaptive

Figure 1 (a) The all-terrain rover Dune built at the University of Salento in collaboration with the Politecnico of Bari; (b) Dune's CAD model



(a)



(b)

suspension allowing the wheels to adjust passively their inclination angle in order to hold a perpendicular posture with respect to the ground.

In the remainder of this paper, Section 2 describes rover modeling techniques for kinematic and dynamic analysis. Dune's mobility characteristics are evaluated and compared with those of a vehicle, equipped with a conventional spring-type suspension, in Section 3. Then, Section 4 introduces the proposed wheel cambering mechanism along with its synthesis and optimization. Finally, relevant conclusions are drawn in Section 5.

2. Rover modelling

In this section, two rover modeling techniques are presented and described. The first is a kinematic model for articulated mobile robots. The second is a quasi-static model of forces acting on the rover. Note that quasi-static models are appropriate due to the relative low speed of those vehicles.

2.1 Rover kinematic model

Kinematic analysis is an important aspect of mobility prediction. In previous research by the authors (Foglia and Reina, 2008), the complete kinematics characterization of a rover was presented. Here, we only recall the inverse kinematic model that involves computing the orientation of the rover and the configuration of its suspension system, given the shape of the terrain and the position of the robot. To this aim, a wheel-terrain contact model must be first defined. It is assumed that each wheel makes contact with the ground at a single point, denoted with P_i , $i = 1, \dots, 4$. This is a reasonable assumption for vehicles with rigid wheels (such as currently planned Mars rovers) moving on firm terrain. For vehicles moving on deformable terrain, distributed wheel-terrain contact stresses can be resolved to resultant forces at a single point.

In general, a wheel-terrain contact force exists at each point P_i and is denoted with $f_i = [f_{t,i}, f_{l,i}, f_{n,i}]^T$ (see Figure 2(a), for a planar schematization). The vector is expressed in the wheel-ground contact frame, and can be decomposed into a tractive and lateral force $f_{t,i}$ and $f_{l,i}$, and a normal force $f_{n,i}$, respectively, tangent and normal to the wheel-terrain contact plane. It is assumed that there are no moments acting at the wheel-terrain interface. The angle γ_i measures the inclination between the horizontal and the wheel-terrain contact plane i .

For a vehicle with m contact points, $m - 1$ loop closure equations can be written. When considering the rover shown in Figure 2(b), these equations can be obtained as:

$$P_4^z = P_3^z - \cos \phi \cdot (2 \cdot l \cdot \sin \beta_R + R \cdot (\cos \lambda_4 - \cos \lambda_3)) \quad (1)$$

$$P_4^z = P_2^z - \cos \phi (t \cdot (\cos \beta_R - \cos \beta_L) + l \cdot (\sin \beta_R - \sin \beta_L) + R \cdot (\cos \lambda_4 - \cos \lambda_3)) - 2w \cdot \sin \phi \quad (2)$$

$$P_4^z = P_1^z - \cos \phi (t \cdot (\cos \beta_R - \cos \beta_L) + l \cdot (\sin \beta_R + \sin \beta_L) + R \cdot (\cos \lambda_4 - \cos \lambda_3)) - 2w \cdot \sin \phi \quad (3)$$

where P_i^z refers to the z component of the wheel contact point i , ϕ and θ are the roll and the pitch of the robot, β_R and β_L are the right and left rocker arm angles, R is the radius of the wheel, and l , w and t are geometric parameters, as explained in Figure 2(b). Due to the presence of the differential gearbox, an additional equation can be written relating the pitch θ to the right and left rocker angle, β_R and β_L , respectively:

$$\theta = \frac{\beta_R + \beta_L}{2} \quad (4)$$

In summary, inputs to the inverse kinematics problem are the terrain elevation map (i.e. P_i and γ_i for each wheel), the position of the rover center, and the rover heading ψ . Position and heading are taken as inputs since the goal of kinematic analysis is often to predict the traversability and stability at a given point in the terrain map. These inputs reduce the number of unknown parameters to four (ϕ , θ , β_R and β_L), which can be determined by solving the nonlinear system of equations (1)-(4).

2.2 Rover force analysis

Force analysis is another important aspect of the rover mobility prediction. The speed of autonomous vehicles is generally limited on rough terrain in order to avoid shocks and for safety reasons. Furthermore, the onboard computational burden is usually quite high (due for example to image processing, path planning or obstacle avoidance) whereas the available processing power is limited. This requires the rover to move slowly in a range of speeds (typically 5-20 cm/s) and accelerations (typically 0.05-0.1 percent of g) where the dynamic contributions can be neglected and a quasi-static model can be deemed appropriate. Figure 3 is a schematic of a four-wheel mobile

Figure 2 (a) Wheel-terrain contact model (plane schematization) and (b) Dune's coordinate frames and nomenclature

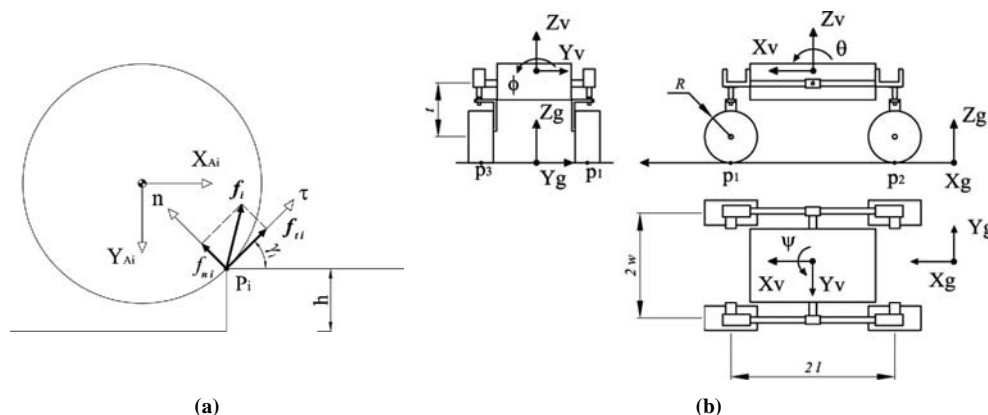
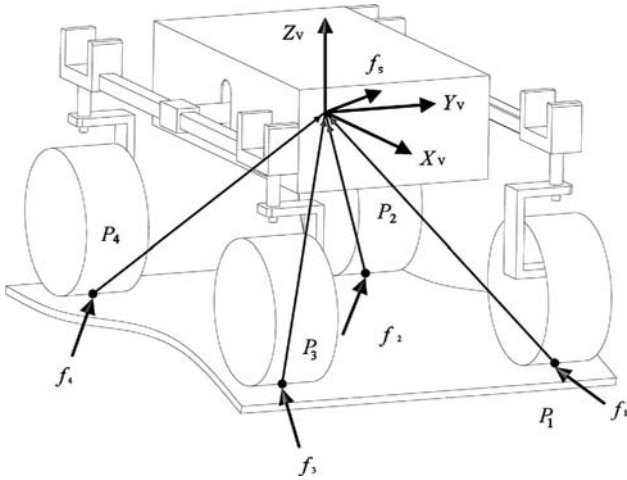


Figure 3 Force analysis for a four-wheeled rover



robot on uneven terrain. The vectors f_i represent the wheel-ground interaction forces. The position vectors p_i are directed from the wheel terrain contact points to the rover center of mass. The vector f_s at the rover center of mass represents the summed effects of gravitational forces, inertial forces, and forces due to interaction with the environment. Note that rover links, wheel and body masses are lumped at the center of mass. A set of quasi-static force balance equations for the rover shown in Figure 3 can be written as:

$$\begin{bmatrix} I & \dots & I \\ 0 & -p_1^z & p_1^y & 0 & -p_4^z & p_4^y \\ p_1^z & 0 & -p_1^x & \dots & p_4^z & 0 & -p_4^x \\ -p_1^y & p_1^x & 0 & & -p_4^y & p_4^x & 0 \end{bmatrix} \cdot \begin{bmatrix} f_1 \\ \vdots \\ f_4 \end{bmatrix} = f_s \quad (5)$$

where I represents a 3×3 identity matrix. This set of equations can be written in compact matrix form as:

$$G \cdot x = f_s \quad (6)$$

Equation (10) is usually referred to as the force distribution equation (Kumar and Waldron, 1988). It consists of a set of six equations in twelve unknowns. Thus, the force analysis problem is under constrained and there exists an infinite set of f_i that balances the body vector f_s . In general, a system with m contact points possesses $2(m - 1)$ degrees of redundancy. Solution methods of the distribution equations have proposed in literature, where a solution x is found that optimizes a user-defined criteria. In order to reproduce the physical behavior of the robot, the optimization criterion should reflect the control strategy implemented onboard. For example, in Iagnemma and Dubowsky (2004) and Thueer *et al.* (2006), a solution to maximize traction was obtained by imposing equal friction coefficients on all wheels. The idea was to have the ratio of tangential and normal forces (Figure 2(a)) as low as possible by selecting the correct set of torques. However, direct measurement of the normal forces and the contact angles is difficult, making a similar control strategy very expensive in practice. In this paper, an optimization approach is proposed, based on the indirect estimation of the tangential forces,

through the measurement of the electrical currents drawn by the wheel drive motors (Ojeda *et al.*, 2006) that can be easily implemented using inexpensive on-board ammeters. A crucial problem for over-constrained rovers is that each wheel is controlled independently in a closed-loop manner. This results in one wheel speeding up while another wheel slowing down to get up to its speed set point under different loading profiles. One way to reduce slippage is that of minimizing the difference between the tractive efforts exchanged by the robot's wheels with the ground. Then, an objective function for the optimization of equation (6) can be defined as:

$$O_1 = \min \left(\sum (f_{i,i}^w - \bar{f}_i)^2 \right) \quad (7)$$

where $f_{i,i}^w$ is the x -component of f_i in the wheel reference frame A_i (Figure 2(a)), and \bar{f}_i is the mean of all $f_{i,i}^w$. In general, the smaller the objective function, the lower the likelihood of slippage. We can formally state the optimization problem as follows: minimize O_1 subject to the equality constraint (6) and to the physical constraints of the system. One such constraint is that all rover wheels should remain in contact with the terrain. This can be expressed by ensuring that all wheel-terrain normal forces $f_{n,i}$ remain positive:

$$f_{n,i} > 0 \quad i = 1, \dots, 4 \quad (8)$$

The second constraint is that the wheel torques must remain within the saturation limits of the actuator:

$$\tau_{\min} < (f_{t,i} \cdot R) < \tau_{\max} \quad i = 1, \dots, 4 \quad (9)$$

The third is that the tractive force exerted on the terrain must not exceed the maximum force that the terrain can bear. The simplest approximation of this constraint is a Coulomb friction model:

$$f_{t,i} < \mu \cdot f_{n,i} \quad i = 1, \dots, 4 \quad (10)$$

where μ is the wheel-terrain force coefficient. This approximation is reasonable for wheels traveling over firm terrain. For a wheel traveling on deformable terrain, the maximum shear strength of the terrain can be computed by the Coulomb-Mohr theory as:

$$F_{\max} = A \cdot (c + \sigma \cdot \tan \phi_t) \quad (11)$$

where A is the wheel contact patch, c is the terrain cohesion, σ is the normal stress at the wheel-terrain interface, and ϕ_t is the internal friction angle (Wong, 2001). Thus, the terrain strength constraint can be written for deformable terrain as:

$$f_{t,i} < F_{\max} \quad i = 1, \dots, 4 \quad (12)$$

Failure to find a vector x that satisfies (6) implies that the rover cannot move in the direction of desired motion. Conversely, a large space of solution for x implies that the terrain is highly traversable.

3. Mobility evaluation

The locomotion performance of Dune is compared via simulations with a geometrically equivalent vehicle that employs a spring-type suspension. For simplicity, the comparative suspension is modeled as composed of four linear spring elements that constraint the wheels to move vertically

with respect to the vehicle frame, as shown in the schematic of Figure 4. The spring rate is chosen to ensure a wheel travel of 35 percent of wheel radius under nominal working conditions, i.e. robot traveling on flat surface. This is a typical value for off-road applications (Wong, 2001).

The locomotion ability of the two architectures is evaluated based on the following metrics:

- Drive motor torque: the higher the torque, the bigger the drive motor, which adds weight to the rover and consumes more energy.
- Wheel load ratio: it is defined as the percentage ratio of the vertical load acting on a single wheel to the total weight force of the robot. Since the tractive thrust that a wheel can develop increases with its vertical load, the higher the load ratio, the larger its traction ability.
- Friction coefficient: it is defined as $\mu = (f_t/f_n)$. The smaller the friction required by the vehicle for a given configuration, the better the climbing ability of the system.

The climbing ability of the suspension mechanisms is very important in the context of all-terrain rovers. Therefore, the behavior of the two types of architecture is studied during the traverse of a rock, when one of the rover's wheels, i.e. left front Wheel 1, rises higher than the other three wheels that remain in contact with the ground. For simplicity, the rock is modeled as a step-obstacle, which, however, represents a worst-case condition. The height of the rock is initially set as half of the wheel radius ($h = 50$ mm). Inputs to the simulations are the z -components of the wheel contact points P_i and contact angles γ_i . First, the inverse kinematic problem, expressed by equations (1)-(4), is solved, then, the correspondent wheel contact forces are evaluated using (6) constrained with the slip minimization-based optimization. The set of geometric and mass parameters used in the simulation and referring to the robot Dune are collected in Table I. Figure 5 shows the variation of the contact angle γ_1 , during the climbing stage (refer to Figure 2(a) for more details). The initial peak γ_1^{\max} corresponds to Wheel 1 in contact with the vertical wall of the step:

$$\gamma_1^{\max} = \arccos\left(1 - \frac{h}{R}\right) \quad (13)$$

whereas γ_1 nulls out when Wheel 1 reaches the top of the step. The simulation results are shown in Figures 6 and 7.

Figure 4 Schematic of a robot outfitted with a spring type suspension

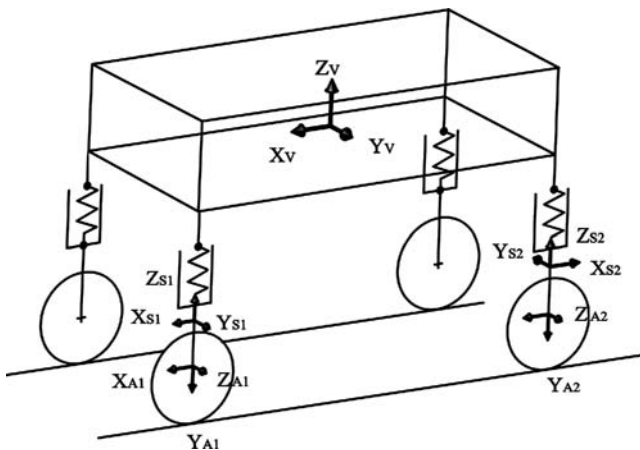
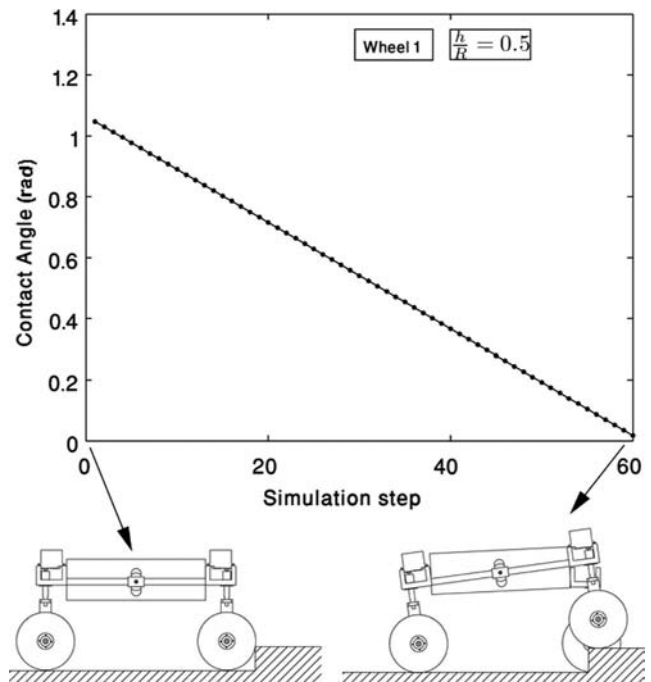


Table I Dune's properties

Dimensions ($2l \times 2w \times t$)	$0.74 \times 0.45 \times 0.32$ m
Wheel diameter	0.20 m
Ground clearance	0.21 m
Total mass	16 kg
Max speed	150 cm/s

Note: See Figure 2 for more details

Figure 5 Change in the contact angle of Wheel 1 during the step-climbing stage

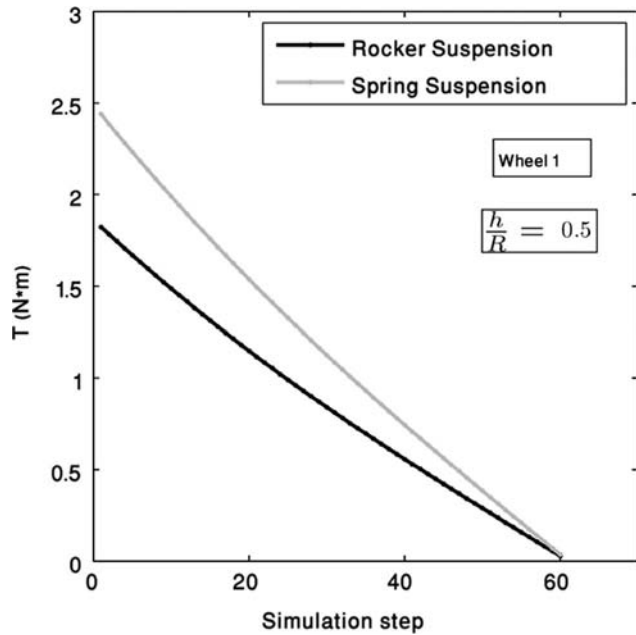


Specifically, the traction torque required by Wheels 1 and 2 (both attached to the left rocker arm) is shown in Figure 6(a) and (b), respectively. Note that these two wheels develop most of the tractive effort, whereas the torques developed by the remaining wheels are negligible and they are omitted here.

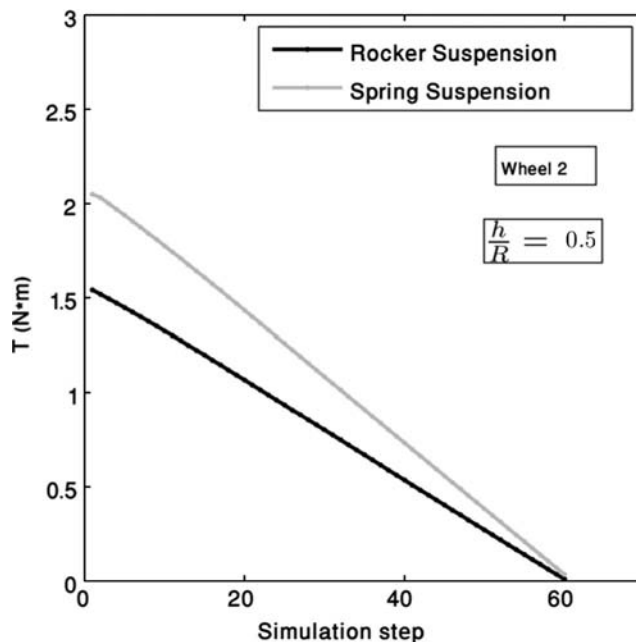
The rocker-type suspension ensures a lower traction torque demand than the spring-type system. This beneficial aspect can be better explained when considering Figure 7, where the change in the load ratio of the four wheels is shown. The rocker-type suspension provides a more uniform weight distribution, whereas, in the spring-type solution, climbing Wheel 1 and cross-coupled Wheel 3 are rapidly loaded, as Wheels 2 and 3 are unloaded accordingly. Thus, the better traction performance of the rocker type suspension is clearly demonstrated. The advantage of the rocker system is confirmed again, when considering the minimum friction coefficient required to traverse the obstacle. If we focus on the worst-case condition at the beginning of the climbing stage, the rocker suspension requires a friction coefficient of $\mu = 0.60$ against a value of $\mu = 0.67$ needed by the spring suspension.

The comparison is further extended by increasing progressively the height of the obstacle up to 300 percent of the wheel radius. We now only refer to the final stage of the climbing maneuver when Wheel 1 has reached the top

Figure 6 Drive torque demand for Wheel 1 (a) and Wheel 2 (b), during step-climbing



(a)



(b)

of the step ($\gamma_1 = 0$). Results are shown in Figure 8 where the change in the wheel load ratio is shown as a function of the obstacle height. The rocker suspension ensures a more even weight distribution. Even with an obstacle high one and half of the wheel diameter ($h = 300$ mm or 300 percent of wheel radius), all wheels still keep contact with the ground and Wheel 1, which results in the “lightest” wheel, retains almost half of its nominal traction ability.

Conversely, when a conventional spring suspension system is employed, obstacles of small dimension result in large variations of weight distribution. Wheel 1 and the rear wheel

of the opposite side, namely Wheel 4, are rapidly loaded while weight is shifted from the remaining two wheels, Wheels 2 and 3, until they lose contact with the ground. This happens for a rock height of about 90 percent of the wheel radius ($h = 88$ mm, marked with a grey dot in Figure 8), when the load ratio for Wheel 2 nulls out, resulting in a reduction of almost half of the overall vehicle tractive power and in an impending rollover instability condition.

In summary, conventional suspension systems greatly reduce the load and therefore the traction on wheels that are extended to lie below the level of the other wheels. The rocker avoids this by featuring a chassis supported on a central pivot, which ensures equal distribution of load on all wheels, and therefore equal traction on each wheel. If a stiff suspension system is used, the chassis will be considerably deflected when any one of the wheel is deflected. A reduction of weight shift may be achieved by using low rate springs. However, this solution would result in an undesirable low oscillation frequency, usually referred to as “too soft a suspension”.

4. Lateral kinematics

One critical drawback of rocker-type suspension is that it does not provide any compensation for the change in the wheel camber angle during suspension travel. This results in a reduction in the overall traction performance of the rover as it conforms to irregular terrain. In this section, a variable camber mechanism is proposed that can be easily integrated with rocker-type suspension systems. The idea is to obtain an adaptive suspension that enables the robot wheels to adjust their inclination angle in order to hold a perpendicular posture with respect to the ground. This ensures that wheels operate at peak efficiency with a regular pressure distribution and a maximum footprint area at all times. Let us refer again, as a practical scenario, to the obstacle climbing. Figure 9(a) shows the change in roll and pitch angle of the rover as a function of the obstacle height. It is clear the averaging effect due to the mechanical differential that reduces the rover’s pitch to half of the irregularities seen by the rocker arm on the ground. In order to get a better understanding of the rover lateral kinematics, we can now plot the roll angle ϕ as a function of the relative rotation between the left rocker arm and the robot’s chassis $\beta_L^r = \beta_L - \theta$, as shown in Figure 9(b). Any rotation of the rocker arm with respect to the chassis produces a correspondent roll angle of the robot. In our example, the left rocker rotates clockwise with respect to the robot body to accommodate the upward travel of Wheel 1. The right rocker arm keeps parallel to the ground, instead. This results in a positive roll rotation of the robot and this, in turn, translates into a wheel camber change. Figure 10 shows a real scenario where Dune climbs a 160 mm high obstacle.

According to our model, the robot’s body tilts with a pitch and roll angle in absolute value of 11.5 and 8.5°, respectively. It is apparent the undesired cambering of all four wheels. The contact patches are largely reduced, affecting the ability to exchange tangential forces with the ground, and, thus, to accelerate, brake, balance lateral loads, and climb obstacles. Therefore, a variable camber system, aiming to keep the wheels upright throughout suspension travels, would be greatly beneficial.

Figure 7 Wheel load ratio variation during step-climbing with respect to the nominal vertical load when the robot travels on flat ground, i.e. load ratio = 25 percent

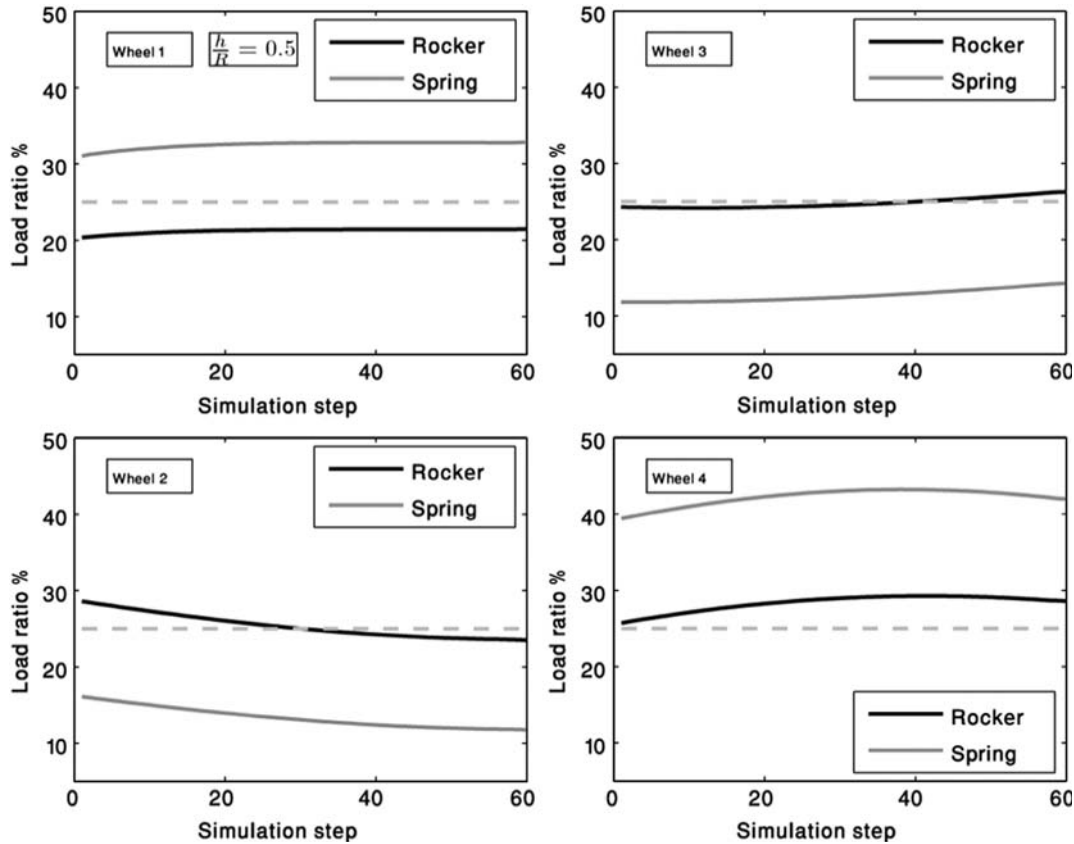
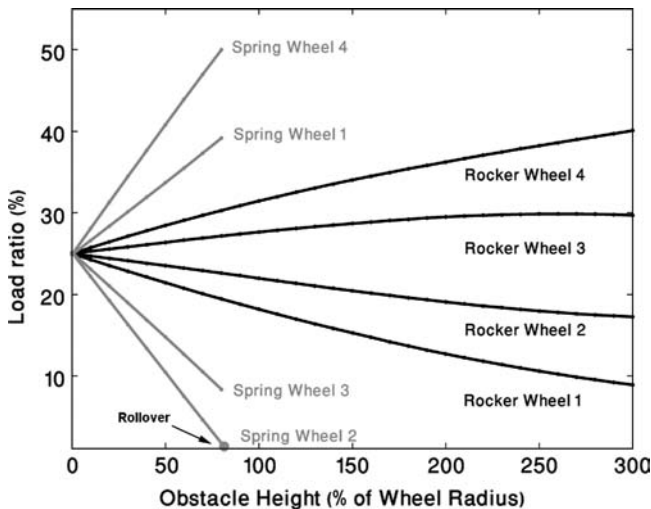


Figure 8 Weight distribution on the four wheels as a function of the obstacle height



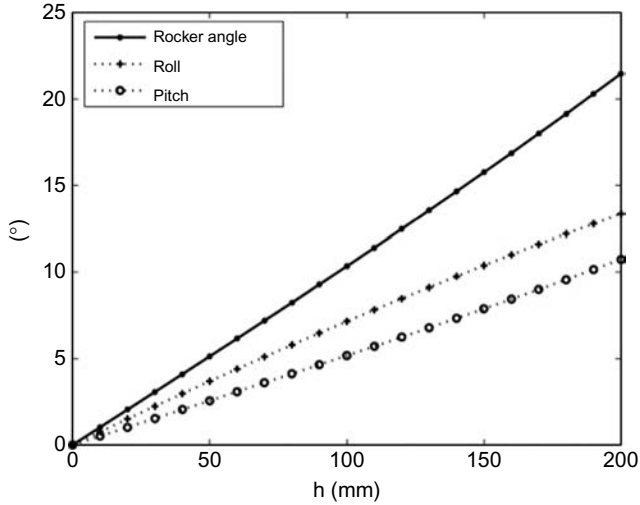
Notes: Black line – rocker-type; Grey line – springtype

4.1 Variable cambering mechanism

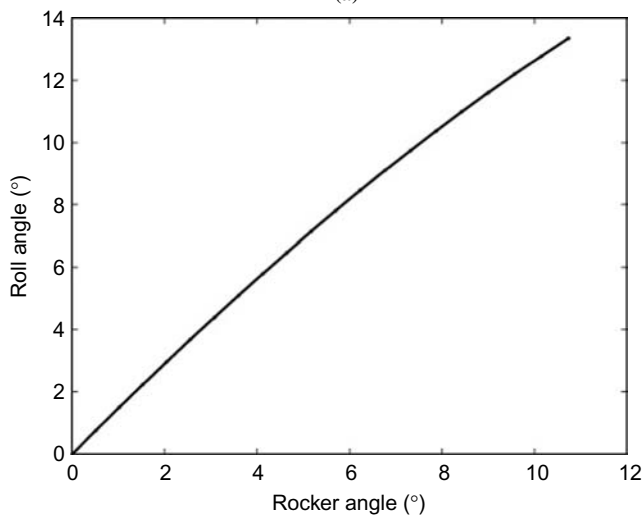
An innovative design of rocker suspension system is proposed that enables the wheels to modify their relative camber to contrast the effect of body roll and to maintain an optimal posture even on highly irregular terrain. This is achieved using a simple driving linkage, which controls the cambering

motion of the wheels of the same side of the robot during relative rotations with respect to the chassis. The adaptive rocker suspension is shown in the CAD drawing of Figure 11. In contrast with the rigid connection of the original design (compare with Figure 1(b)), each rocker arm is now attached to the semi-axis of the differential via a revolute joint, which allows it to pivot around its longitudinal axis, modifying the camber angle of the attached wheels. The variable cambering linkage is shown in more detail in the close up inset of Figure 11. Links 1 and 2 form the driving linkage that controls the wheel inclination change in the left rocker-chassis relative motion. A similar mechanism operates on the right side. Link 1 is attached to Link 2 and to the chassis through two spherical joints, whereas Link 2 is rigidly connected with the rocker arm. Links 1 and 2 serve as crank and coupler of the driving mechanism. This can be better seen when considering the projection of the linkage in the transverse plane of the robot, as shown in Figure 12, which allows one to analytically study the system referring to a simple model without losing much of accuracy. Input to the linkage is the vertical displacement of the slider B that is produced by the rotation of the left rocker link with respect to the robot's body. The linkage reacts by changing the angle of Link 2, i.e. the wheel camber angle, which we can consider as the output of the mechanism. In order to maximize its footprint, each wheel needs to remain upright, perpendicular to the ground, as the suspension complies with terrain unevenness. The proposed mechanism fulfils the design requirement that the wheel gains a positive camber during its upward travel and a negative

Figure 9 (a) Change in the rover rotation as a function of obstacle height; cross-marked line – roll angle; circle-marked line – pitch angle; solid line – left rocker angle; note that pitch angle is negative, but here for comparative reasons its absolute value is plotted and (b) change in the body roll angle as a function of the left rocker-chassis relative rotation



(a)



(b)

camber during downward travel. Wheel camber is assumed equal to zero when the rocker arm is parallel with the body, i.e. perfectly planar ground. This solution features cost-effectiveness, simplicity and requires small and affordable modifications to the conventional rocker suspension design.

Mechanism synthesis

The coupler Link 2 is the driver in the linkage: any relative rotation of the rocker arm with respect to the robot's body produces a correspondent vertical displacement of the slider B:

$$\Delta x_B = \sin \beta_L^r \cdot b \tag{14}$$

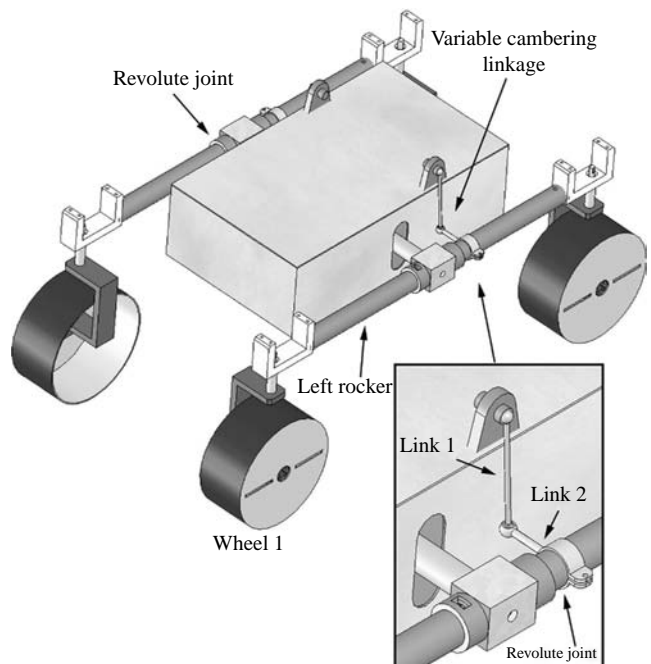
where b is the distance of Link 2 attachment along the left rocker from the differential semi-axis. In order to determine the relationship between Δx_B and the variables θ_1 and θ_2 , as expressed in Figure 12, the position analysis of the mechanism needs to be analytically solved using the closure condition

Figure 10 Traverse of a 160 mm-high obstacle



Note: The large roll of Dune's body and the correspondent wheel camber change

Figure 11 The adaptive rocker suspension system based on a variable cambering mechanism



$(B-O) = (A - O) + (B - A)$. Rewriting in its component equations, one gets:

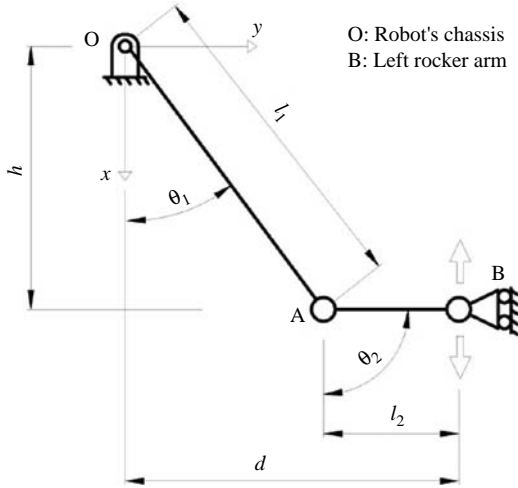
$$l_1 \sin \theta_1 + l_2 \sin \theta_2 = d \tag{15}$$

$$l_1 \cos \theta_1 + l_2 \cos \theta_2 = h + \Delta x_B \tag{16}$$

By squaring both sides of (15) and (16), adding and rearranging the result, it is possible to get an explicit equation of θ_2 as a function of the system input:

$$k_1 \cdot \cos \theta_2 + k_2 \cdot \sin \theta_2 + k_3 = 0 \tag{17}$$

Figure 12 Planar schematization of the variable camber mechanism



where:

$$\begin{aligned} k_1 &= 2 \cdot l_2 \cdot (h + \Delta x_B) \\ k_2 &= 2 \cdot d \cdot l_2 \\ k_3 &= l_1^2 - (d^2 + l_2^2 + (h + \Delta x_B)^2) \end{aligned}$$

Equation (17) can be solved using the standard trigonometric identities for half angles, one gets:

$$\begin{aligned} (k_3 - k_1) \cdot t^2 + 2 \cdot k_2 \cdot t + (k_1 + k_3) &= 0 \quad (18) \\ t &= \tan\left(\frac{\theta_2}{2}\right) \end{aligned}$$

Finally, solving for t gives:

$$t = \frac{-k_2 + \sigma \sqrt{k_2^2 - k_3^2 + k_1^2}}{k_3 - k_1} \quad (19)$$

where $\sigma = -1$ is a sign variable identifying the assembly mode. There are two solutions for θ_2 corresponding to the two values of σ . These correspond to two assembly modes for the linkage. Note that the variable t may be complex when $(k_1^2 + k_2^2 < k_3^2)$. If this happens, the mechanism cannot be assembled. After θ_2 is known, equations can be solved for θ_1 . Dividing (15) by (16) and solving for θ_1 gives:

$$\theta_1 = \arctan\left(\frac{d - l_2 \sin \theta_2}{h + \Delta x_B - l_2 \cos \theta_2}\right) \quad (20)$$

Equations (19)-(20) give a complete and consistent solution to the position problem as a function of the geometrical parameters l_1, l_2 and b and the input variable β_L^r . Note that the value of θ_2 at rest is set to $\theta_2^0 = 90^\circ$, and d is a known geometrical parameter ($d = 0.065$ m for the rover Dune). Finally, given θ_2 , the wheel camber of Wheels 1 and 2 that are attached to the left rocker can be obtained as:

$$\gamma_c^L = \frac{\pi}{2} - \theta_2 \quad (21)$$

The driving linkage is to be synthesized in order that the coupler will move through an angle θ_2 satisfying a given function. This type of synthesis approach is usually referred to as function generation problem. The functional relationship between the two variables β_L^r and θ_2 can be generally expressed as:

$$f(\beta_L^r, \theta_1, \theta_2, l_1, l_2, b) = 0 \quad (22)$$

where l_1, l_2, b are design variables defining the system geometry. Our goal is to design the system to minimize the cost function:

$$g(\beta_L^r, \theta_2) = \phi(\beta_L^r) - \gamma_c^L(\theta_2) \quad (23)$$

where the function $\phi = \phi(\beta_L^r)$ is shown in Figure 9(b). This optimization problem can be solved using a least-square approach, yielding to the following results: $l_1 = 0.1$ m, $l_2 = 0.054$ m, $b = 0.071$ m. The camber change of Wheels 1 and 2 as a function of the left rocker relative rotation β_L^r obtained with this geometry is shown in Figure 13. It is clear how the cambering mechanism counteracts with good accuracy the robot's roll, helping the wheels to keep the correct posture. The discrepancy with the desired function can be expressed as absolute average of the residuals and results in $RES = 0.81^\circ$. If the analysis is limited to the usual operating range of the rover, i.e. roll angle between $[-10 \ 10]^\circ$ ($\beta_L^r \in [-7 \ 7]$ deg) and obstacle height h between $[-150 \ 150]$ mm, the residuals decrease to $RES = 0.53^\circ$, showing a very close agreement and attesting to the feasibility of this approach. Finally, Figure 14(b) shows the configuration of the adaptive rover for the step climbing condition previously considered in Figure 10. Using the wheel cambering mechanism, each wheel keeps unaltered its footprints even in presence of substantial body roll. This condition cannot be achieved with a normal rocker suspension, as shown in Figure 14(a). This result was achieved under the assumption of a flat-top obstacle. However, the cambering mechanism would be beneficial even in presence of a not-leveled obstacle by keeping a suboptimal posture of the three not-climbing wheels.

5. Conclusions

This paper evaluated the locomotion performance of a robot endowed with advanced mobility features to traverse natural terrain. The vehicle adopted an independently controlled four-wheel-drive/four-wheel-steer architecture, and employed a passive rocker-type suspension to improve its ability to climb up obstacles, while ensuring good traction and

Figure 13 Wheel camber change as a function of left rocker relative angle using the adaptive suspension system

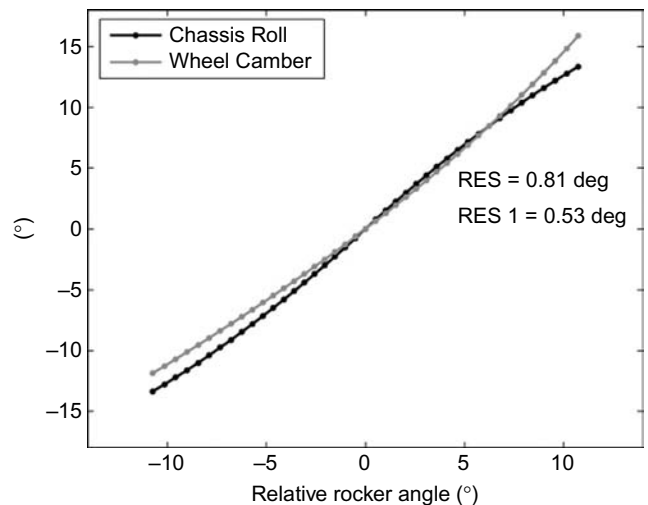
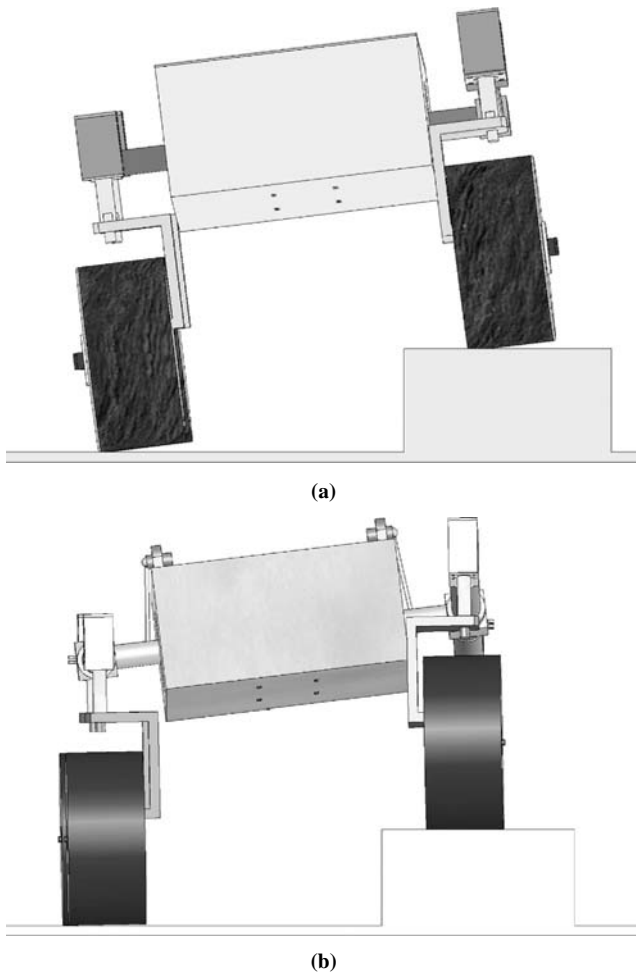


Figure 14 Comparison between the normal rocker suspension (a), with the adaptive alternative (b)



stability performance. A comparison with a conventional vehicle adopting a spring-type suspension was performed through simulations, showing its advantages and overall better performance.

An adaptive suspension system with wheel cambering compensation was also presented that can be integrated with rovers employing rocker-type suspensions. The geometrical optimization of the variable cambering mechanism was discussed, aimed to keep wheels always perpendicular to the ground as the robot tilts adapting to ground unevenness.

References

- Bickler, D. (1989), US Patent Number 4,840,394 – Articulated Suspension Systems, US Patent Office, Washington, DC.
- Bickler, D. (1998), “Roving over Mars”, *Mechanical Engineering Magazine*, April, American Society of Mechanical Engineers.
- Foglia, M. and Reina, G. (2008), “Locomotion performance evaluation of an all-terrain rover”, *International Journal of Mechanics and Control*, Vol. 9 No. 2, pp. 13–25.

- Gillespie, T. (1992), *Fundamentals of Vehicle Dynamics*, SAE, Warrendale, PA.
- Iagnemma, K. and Dubowsky, S. (2004), *Mobile Robots in Rough Terrain: Estimation, Motion Planning, and Control with Application to Planetary Rovers*, Springer, Berlin.
- Kumar, V. and Waldron, K. (1988), “Force distribution in closed kinematic chains”, *IEEE Transactions on Robotics and Automation*, Vol. 4 No. 6, pp. 657–64.
- Lindemann, R. and Voorhees, C. (2005), “Mars exploration rover mobility assembly design, test and performance”, *IEEE Conf. Syst. Man, Cybern., New Orleans, LA*, pp. 450–5.
- Maimone, M., Johnson, A., Willson, R. and Matthies, L. (2004), “Autonomous navigation results from the Mars exploration rover (MER) mission”, paper presented at Intern. Symp. Experimental Robot, Singapore.
- Ojeda, L., Reina, G., Cruz, D. and Borenstein, J. (2006), “The FLEXnav precision dead-reckoning systems”, *International Journal of Vehicle Autonomous Systems (IJVAS)*, Vol. 4 Nos 2–4, pp. 173–95.
- Quaglia, G., Bruzzone, L., Bozzini, G., Oderio, R. and Razzoli, R. (2011), “Epi. q-TG: mobile robot for surveillance”, *Industrial Robot: An International Journal*, Vol. 38 No. 3, pp. 282–91.
- Reina, G., Ojeda, L., Milella, A. and Borenstein, J. (2006), “Wheel slippage and sinkage detection for planetary rovers”, *IEEE/ASME Transactions on Mechatronics*, Vol. 11 No. 2, pp. 185–95.
- Remy, D., Baur, O., Latta, M., Lauber, A., Hutter, M., Hoepflinger, M.A., Pradalier, C. and Siegwart, R. (2011), “Walking and crawling with ALoF: a robot for autonomous locomotion on four legs”, *Industrial Robot: An International Journal*, Vol. 38 No. 3, pp. 264–8.
- Rohmer, E., Reina, G. and Yoshida, K. (2010), “Dynamic simulation-based action planner for a reconfigurable hybrid leg-wheel planetary exploration rover”, *Advanced Robotics*, Vol. 24 Nos 8/9, pp. 1219–38.
- Sandin, P. (2003), *Robot Mechanisms and Mechanical Devices*, McGraw-Hill, New York, NY.
- Schäfer, B., Gibbesch, A., Krenn, R. and Rebele, B. (2010), “Planetary rover mobility simulation on soft and uneven terrain”, *Journal of Vehicle System Dynamics*, Vol. 48, pp. 149–69.
- Thuerer, T., Krebs, A. and Siegwart, R. (2006), “Comprehensive locomotion performance evaluation of all-terrain robots”, paper presented at IEEE/RSJ Inter. Conf. on Intelligent Robots and Systems, Beijing, China.
- Thuerer, T., Krebs, A., Lamon, R. and Siegwart, S. (2007), “Performance comparison of rough-terrain robots – simulation and hardware”, *Journal of Field Robotics*, Vol. 24 No. 3, pp. 251–71.
- Wong, J. (2001), *Theory of Ground Vehicles*, Wiley-Interscience, New York, NY.
- Wong, J. and Huang, W. (2006), “Wheels vs. tracks – a fundamental evaluation from the traction perspective”, *Journal of Terramechanics*, Vol. 43, pp. 27–42.

About the authors

Dr Giulio Reina received the Laurea degree and the Research Doctorate degree from the Politecnico of Bari, Italy in 2000 and 2004, respectively, both in Mechanical Engineering.

From 2002 to 2003, he worked at the University of Michigan Mobile Robotics Laboratory as a Visiting Scholar. In 2007, he was awarded a Japanese Society for Promotion of Science (JSPS) fellowship for a one-year research at the Space Robotics Laboratory of the Tohoku University, Sendai, Japan. In 2010, he was also selected to receive an Endeavour Research Fellowship at the Australian Centre for Field Robotics of the University of Sydney, Australia. Currently, he is an Assistant Professor in Applied Mechanics with the Department of Engineering for Innovation, University of Salento, Lecce, Italy. His research interests include mobile robotics for planetary exploration, mobility and localization on rough-terrain, computer vision

applied to robotics, and agricultural robotics. Giulio Reina is the corresponding author and can be contacted at: giulio.reina@unisalento.it

Mario Foglia received the Laurea and Research Doctorate degrees in Mechanical Engineering from the Politecnico of Bari, Italy in 1995 and 2000, respectively. Since 2000, he has been an Assistant Professor at the Department of Mechanical and Management Engineering, Politecnico of Bari. His research interests include path planning, agricultural robotics and localization and kinematic design of mobile robots.